



Article Type: Research Article

Received: 30/10/2020

Published: 16/12/2020

DOI: 10.46718/JBGSR.2020.06.000144

## Monosaccharide Degradation Analysis by Functional Density Theory at Level B3lyp/6-311 G (D, P)

Ablé Anoh Valentin, N'guessan Boka Robert and Bamba El-Hadji Sawaliho\*

Laboratory of Constitution and reaction of matter, UFR-SSMT, Félix Houphouët-Boigny University, Ivory Coast

\*Corresponding author: Bamba El-Hadji Sawaliho\*, Laboratory of Constitution and reaction of matter, UFR-SSMT, Félix Houphouët-Boigny University 22 BP 582 Abidjan 22, Côte d'Ivoire, Ivory Coast

### Abstract

This research focuses on the plantain banana. It aims to identify how starch polysaccharides degrade. It targets explaining  $\alpha$ -D-glucose interaction modalities. This compound design amylose or amylopectin subunit. The work uses Functional Density Theory (DFT) at the B3LYP/6-311 G (d, p) level. It includes two aspects. Foremost, it compares the two monosaccharides potential configuration  $\alpha$  and  $\beta$ . It puts in evidence the first one as be the most stable. Secondly, the paper highlights acceptor or donor hydrogen bond (HB) sites. It exploits RSP map data. Thirdly, it computes and analyzes geometric and energetic parameters of three complex. It studies those between amylose subunit and water or carbon dioxide. It also examines the latter reagent role in  $\alpha$ -D-glucose-water. It leads to the following conclusions. Water alters  $\alpha$ -D-glucose through HB into its H11, H15, H18 and O23. Carbon dioxide doesn't interact directly with monosaccharides. However, it consolidates water action in its association with  $\alpha$ -D-glucose.

**Keywords:**  $\alpha$ -D-glucose; amylose; amylopectin; starch; electrostatic potential; interaction; hydrogen bond; DFT

### Introduction

Banana plantain constitutes a staple food for half a billion people [1]. It cultivates in humid intertropical areas. In Côte d'Ivoire, annual production realizes 1.7 million tons. It places it in the third most important crop, after yam and cassava [2]; it contributes to the alimentation security strategy of Côte d'Ivoire; this country deploys various agriculture techniques to improve its fruitfulness. This is growing over the years. However, it doesn't cover population needs; post-production losses remain high, reaching 30% [2] despite the expensive conservation methods used. The research focuses on plantain degradation modalities. The literature provides information on the roles of water, carbon dioxide and temperature. The water in banana pulp contains at least 60% by weight [3]. It interacts easily with its constituents, specifically with the polysaccharides of amylopectin. The plantain storage place should be in an atmosphere with 10% CO<sub>2</sub> [4]. Its small amount prevents it from reacting successfully with a glucose-water complex. It doesn't slow the aqueous breakdown of starch [5]. The deterioration of polysaccharides represents another explanation for its collapse.

Works link banana degeneration to the progressive polysaccharide's biodegradation into tri-saccharides, disaccharides and monosaccharides [6]. They associate this process with amylose or amylopectin hydrolysis by enzymes [7]. More, literature establishes that low temperatures extend plantain duration survival; cold plays an important role in its slowing metabolism [8,9]. The research aims to identify how water or carbon dioxide can alter starch monosaccharides. In other side, leaflet remains silent on the mechanisms underlying this latter degradation. This work proposes to help fill this gap. Its knowledge contributes to defining solutions to maintain amylopectin safe in banana.

This research wants to provide these mechanisms. It analyzes these two reagents binding modalities with  $\alpha$ -D-glucose. In the process, it tests [4] results of relating to carbon dioxide inaction on the latter. It's expanding on its ability to degrade monosaccharide-water complex. After this introduction, the paper presents research methods. In this section, it shows these and calculation level. It recalls the hypotheses connecting to HB. In the third part, it gives and discusses its results. It explicit monosaccharides (AM1G) anomer subunits,  $\alpha$ -D-glucose. It details ESP. It

focuses on AM1G interactions with water. It examines those with carbon dioxide. It presents a case where this latter reacts with AM1G-H<sub>2</sub>O complex. It discusses temperature effects and polysaccharides degradation throughout this article. After, it describes the methods used to deal with these points.

## Research Methods

Calculation methods describe the assumptions of complex HB, geometry and parameters. It incorporates computation modalities and levels of the planned. Gaussian 09 software [10] helps to estimate them.

### Methods and Level of Calculation

This research uses Density Functional Theory (DFT) method [11]. Frequency calculations follow molecular geometry optimization systematically. Physical quantity values exploit B3LYP/6-311 G level (d,p). Furthermore, computations require to specify assumptions about HB.

### Assumptions about HB

HB results from an attractive interaction between hydrogen and an acceptor (HBA) atom. Its geometry and energy parameters characterize it. Hydrogen has a covalent link with a strongly electronegative donor (HBD) such as nitrogen. HBA can belong to the same molecule or to a neighbouring one, oxygen, fluorine or carbon.

### Main Geometric Parameters

Microwave and rotational spectroscopy allow describing chemical entities gas [12]. Neutron X-ray diffraction and NMR help to obtain its elements in the solid state. Fourier Transform Infrared Spectroscopy enables disposing of those in the liquid phase [13]. (Figure 1) shows the main geometric

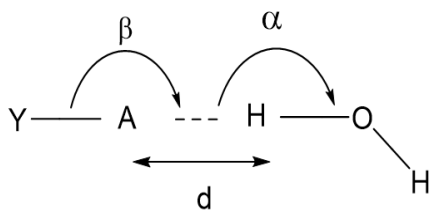


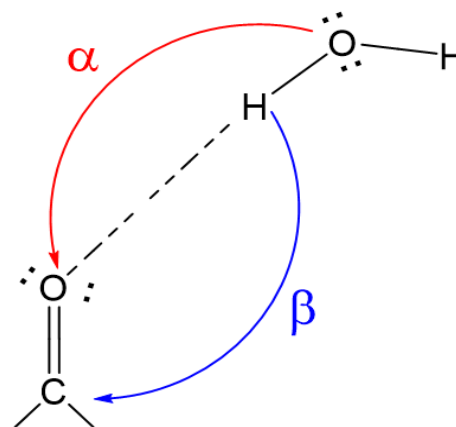
Figure 1: Geometric parameters  $d$ ,  $\alpha$ ,  $\beta$  illustrating an H-link.

parameters. Angles  $\alpha$  and  $\beta$  define linearity degree between OH axis and Y-A link or an approach direction [14]. H... A represents the length interaction  $d$  between H and HBA. X-H means the covalent (polarized) bond, between the HBD atom X and H. The parameters  $d$ ,  $\alpha$  and  $\beta$  specify the geometry of the HB [15]. This is stronger when X, H and A are aligned. Moreover, calculation hypothesis also concerns

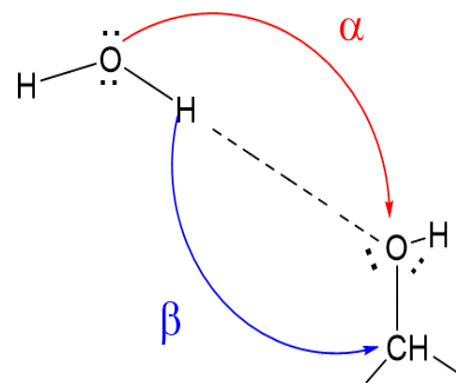
the complex before its optimization.

### Main Complex Geometric Parameters Before Optimization

HB creation requires HBD presence and HBA; water and AM1G represent them respectively. HBD and HBA ripe approach distances refer to minimal electronic energy. Before any optimization, the linearity angle  $\alpha$  is  $180^\circ$ . The direction one  $\beta$  is  $109.5^\circ$  for  $sp^3$  hybridized oxygen and  $120^\circ$  for  $sp^2$  one (Figure 2). More, O-H is 2 Å. The values correspond to a strong HB [16].



a: Oxygen  $sp^3$   
 $\alpha=180^\circ$ ;  $\beta=109.5^\circ$



b: Oxygen  $sp^2$   
 $\alpha=180^\circ$ ;  $\beta=120$

Figure 2: ESP linearity and direction angles definition.

### Energy Parameters Calculation

Equation (1) illustrates AM1G complexation reaction.



Where: M = AM1G and X = H<sub>2</sub>O or CO<sub>2</sub>.

The interaction energy ( $\Delta E$ ) corresponds to the difference between that of complex MX and its subunits M and X. Its calculation bases on the relation [2]:

$$\Delta E = E_{\text{compM1G + Water/E CO}_2\text{+ EBSSE}} - E_{\text{H-X}} \quad \text{Equation 2}$$

Interaction energy equals subtraction:

- Each specie energy from that of AM1G and water, when the structure contains two entities;
- Each specie energy from that of AM1G, water and carbon dioxide, for a system with three components.

Gaussian 09 software [10] measures BSSE directly (Basis Set Superposition Error) energy. The HB between HBD H-X and HBA Y-A groups characterize by the reaction:



The complex Y-A  $\cdots$  H-X represents its product. Equation 4 allows calculating the change in electronic energy at 0 K.

$$\Delta E_{\text{elec}}^0 = E_{\text{elec}}^0(Y-A \cdots H-X) - [E_{\text{elec}}^0(Y-A) + E_{\text{elec}}^0(H-X)] \quad \text{Equation 4}$$

The internal energy at 298.15 K obtains by summing the electronic, rotational, translational and vibrational ones [17]

$$\Delta E_{298}^0 = \Delta E_{\text{electronique}}^0 + \Delta E_{\text{(rotation)}}^0 + \Delta E_{\text{translation}}^0 + \Delta E_{\text{vibration}}^0 \quad \text{Equation 5}$$

The optimization of reagent and product geometry provides the values for electronic and vibrational energies. It allows obtaining those related to the nuclear drive. The approximation of the perfect gases enables calculating rotation and translation ones (equation 6):

$$\Delta E_{\text{translation}}^0 = \Delta E_{\text{(rotation)}}^0 = -3/2 RT \quad \text{Equation 6}$$

$\Delta E_{\text{vibration}}^0$  incorporates ZPVE (Zero Point Vibrational Energy). This corresponds to the lowest vibration energy of the 3N-6 normal modes (3N-5 for linear molecules). Each has a frequency  $\nu_i$ . The additional energy  $\Delta E_{\text{(vib.thermal)}}^0$  related to the temperature increase from 0 to 298.15K (equation 7)

$$\Delta E_{\text{(vib.thermal)}}^0 = R \sum_{i=1}^{(3N-6)} \left[ \frac{h\nu_i/k}{(e^{(h\nu_i/298K)}) - 1} \right] \quad \text{Equation 7}$$

The internal energy variation at 298.15 K becomes (equation 8):

$$\Delta E_{298}^0 = \Delta E_{\text{elec}}^0 + \Delta ZPVE + \Delta E_{\text{(vib.thermal)}}^0 - 3RT \quad \text{Equation 8}$$

Equations (9) and (10) provide the enthalpy and free enthalpy variations, respectively, at 298.15 K related to the formation of the complex Y-A  $\cdots$  H-X.

$$\Delta H_{298K}^0 = \Delta E_{298K}^0 + RT \quad \text{Equation 9}$$

$$\Delta G_{298K}^0 = \Delta H_{298K}^0 - T\Delta S_{298K}^0 \quad \text{Equation 10}$$

$\Delta S_{298K}^0$  denotes the entropy variation (equation 11) [18,19]:

$$\Delta S_{298K}^0 = \Delta S_{\text{trans}}^0 + \Delta S_{\text{rot}}^0 + \Delta S_{\text{vib}}^0 \quad \text{Equation 11}$$

The exploitation  $\alpha$  of equations 4 to 9 leads to different energies values. It allows discussing the  $\alpha$ -D-glucose HB sites. It analyzes complex stability.

## Results and Discussions

This part presents two calculations results. It explicates those about the anomers. It also shows  $\alpha$ -D-glucose geometric and energy parameters. These concern situations where this molecule is isolated or associated with the water or carbon dioxide.

### $\alpha$ -D-glucose anomers studies

Anomers are differentiated by  $\alpha$  and  $\beta$ . For  $\alpha$ , OH group is oriented downwards (or to the right in a linear representation). The form becomes  $\beta$  when OH is at the top (or to the left). Banana preliminary study in a gaseous medium (under vacuity) remains essential to determine its starch degradation in a liquid one. (Table 1) shows  $\alpha$ -D-glucose  $\alpha$  and  $\beta$  optimization energies in the first state at level DFT/B3LYP/6-311G (d, p).

This latter parameter presents a small difference of 0.21 kcal/mol; the cycle composition stays identical. However, the alpha form appears relatively more stable in a vacuum. Its study also incorporates an electrostatic potential analysis.

### $\alpha$ -D-glucose electrostatic potential study

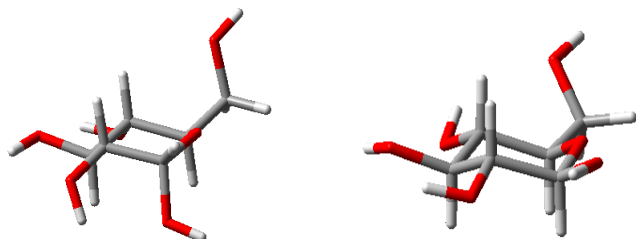
The surface represents molecule electrostatic potential (ESP) studies. In (Figures 3-5), red colour indicates the most negative. The blue one corresponds to most positive charges. Equation 12 gives electron density [7]:

$$\rho = 1 / (2 \left[ (3\pi^2)^{1/3} \right] |\nabla \rho| / \rho^{4/3}) \quad \text{Equation 12}$$

The ESP map shows three sites in blue. These

**Table 1:** Gaseous Glucose  $\alpha$  and  $\beta$  Optimization Energies at Level DFT B3LYP 6311G (d,p).

Optimization energy		
$\alpha$ -D-glucose	-687,366963 a.u	-431,343.39 kcal/mol
$\beta$ -D-glucose	-687.366631 a.u	-431,343.18 kcal/mol



Form  $\alpha$

Form  $\beta$

Figure 3 : D-glucopyrano representation.

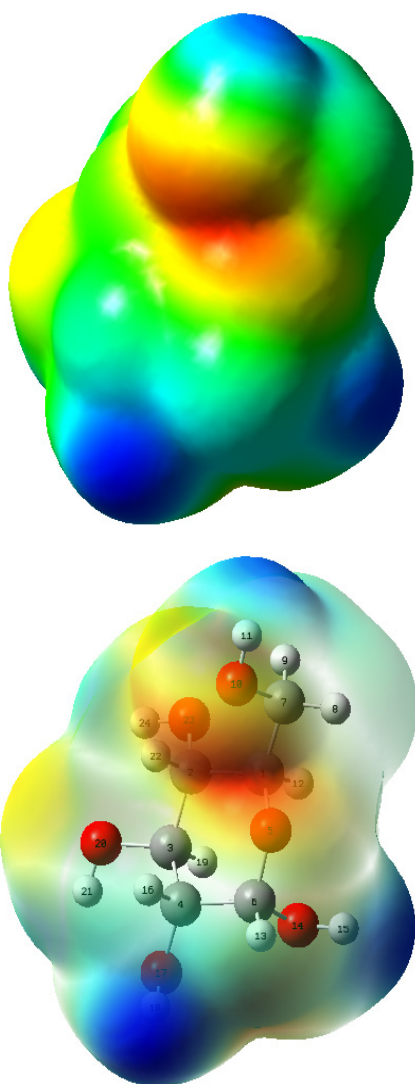


Figure 4:  $\alpha$ -D-glucose ESP Map.

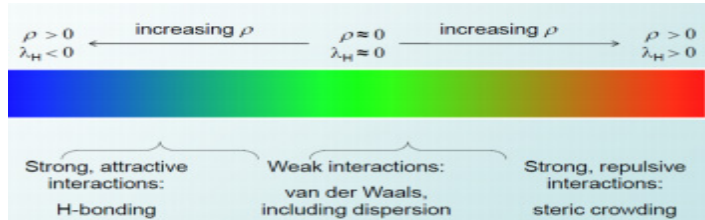


Figure 5: Molecular interactions on schematic diagram as density function or arbitrary coordinate ( $\lambda_H$ ).

can react with a nucleophile; their atoms become able to participate in a HB. They comprise the oxygen bound to the carbons at anomeric position 1 or 2. The two others are on methoxide or seated at rank 6. These sites constitute  $\alpha$ -D-glucose polymerization centre. Their stance knowledge opens the way to analyzing its interaction with water then with carbon dioxide (Figure 6).

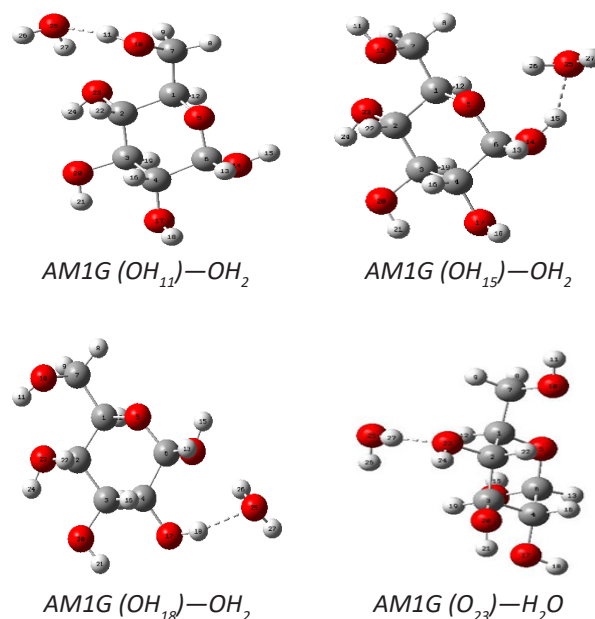


Figure 6:  $\alpha$ -D glucose hydrogen bonding illustration with water.

#### AM1G-OH<sub>2</sub> complex study

The article presents AM1G-OH<sub>2</sub> complex geometric parameters. It sets the linearity angle  $\alpha$  to  $180^\circ$  and the direction  $\beta$  to  $109.5^\circ$  (hybrid oxygen sp<sup>3</sup>) before optimizing it.

#### Geometric Parameters

The distance between oxygen and hydrogen at the probe remains to 2 Å. The angle between water OH bonds, noted  $\gamma$  is worth  $109.5^\circ$ . The calculations lead to geometric parameters values collected in (Table 2) These stay insensitive to temperature variations. HB creation doesn't depend on them. The different link lengths obtained

**Table 2** : AM1G- H<sub>2</sub>O Geometric Parameters.

Complex	T = 25 °C				T1 = 13 °C			
	d(Å)	α (°)	β (°)	γ (°)	d(Å)	α (°)	β (°)	γ (°)
AM1G (OH <sub>11</sub> )—OH <sub>2</sub>	1.86	161.68	93.95	105.18	1.86	161.68	93.95	105.18
AM1G (OH <sub>15</sub> )—OH <sub>2</sub>	1.94	146.48	126.38	105.81	1.94	146.48	126.38	105.81
AM1G (OH <sub>18</sub> )—OH <sub>2</sub>	1.89	151.21	109.49	105.72	1.89	151.21	109.49	105.72
AM1G (O <sub>23</sub> H)—H <sub>2</sub> O	1.95	162.99	110.75	104.06	1.95	162.99	110.75	104.06

prove the presence of intermolecular HB between AM1G hydrogen and the water oxygen. They establish another one between this latter hydrogen and O23.

AM1G OH group position changes the geometric parameter values. The distance *d* varies less for the OH of site H<sub>15</sub> and O<sub>23</sub>. It becomes relatively larger for those at H<sub>11</sub> and H<sub>18</sub>. These disparities indicate that HB strengths of the AM1G in the aqueous phase differ according to the hydrogen or oxygen to which these atoms attach; the HB occurs with H<sub>11</sub> and [H]<sub>18</sub>. The weakest associates with H<sub>15</sub> and O<sub>23</sub>. In many complex, angles α and β deviate from their reference values; their HB are unstable. α-D-glucose in the presence of water establishes two types of HB: a strong with H<sub>11</sub> or H<sub>18</sub> and a weak with H<sub>15</sub> or [O]<sub>23</sub>. Moreover, the temperature doesn't modify the geometric parameters (Figures 7).

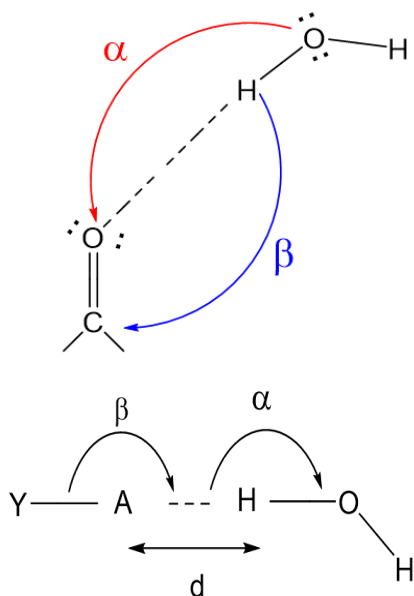


Figure 7

## Energetic Parameters

(Table 3) shows energy values for the different HB. All ΔE<sub>int</sub> are negative. They reflect a solid interaction between water and AM1G. The link is stronger for H11 (ΔE<sub>int</sub> = -8,016 kcal/mol). This result clarifies the confusions related to (Table 2); the distance *d* is shortest for the AM1G (OH<sub>11</sub>)-OH<sub>2</sub>. However, the values from ΔE<sub>int</sub> seem to contradict that of *d* in the (Table 3); they indicate that the interaction is more stable with H<sub>15</sub> than H<sub>18</sub>. In reality, this latter remains the most stable. Eelec energy calculated posits that the complex with H<sub>11</sub> and H<sub>18</sub> are relatively most solid.

They confirm interpretations of the data in (Table 2). More, the temperature hardly modifies the enthalpies of the AM1G complexation reaction (Table 4). On the other hand, it lowers free enthalpies by 28% on average as shown in the (Table 5). Free enthalpies remain negative at 13 °C and 25 °C T. They establish that the reactions associated occur spontaneously. Furthermore, the (Table 3) data suggests that AM1G (OH<sub>11</sub>)-OH<sub>2</sub> has the lowest value. This complex form HB more easily than the others; carbon bound to H<sub>11</sub> become the preferred site. It locates on anomeric oxygen at position 6. According to [20], the low negative enthalpy corresponds to

**Table 3** : AM1G-OH<sub>2</sub> Energetic parameters.

Complex	T = 25 °C					T1 = 13 °C	
	Eélec	ΔE <sub>int</sub>	ΔE <sub>gap</sub>	ΔH (T)	ΔG (T)	ΔH (T1)	ΔG (T1)
AM1G- (OH <sub>11</sub> )— OH <sub>2</sub>	-479,331.538	-8,016	180,151	-12,841	-2,116	12,841	-2,553
AM1G- (OH <sub>15</sub> )— OH <sub>2</sub>	-479,328.400	-7,348	180,616	-9,981	-1,217	-9,995	-1,574
AM1G- (OH <sub>18</sub> )— OH <sub>2</sub>	-479,330.244	-3,270	178,294	-11,499	-1,235	11,501	-1,653
AM1G- (O <sub>23</sub> H)— H <sub>2</sub> O	-479,329.943	-3,664	178,708	-7,307	-1,497	-7,330	-1,903

The work suggests this reaction's mechanism; H<sub>2</sub>O atoms promote HB with H<sub>11</sub>, H<sub>15</sub>, H<sub>18</sub> and O<sub>23</sub>. The strongest occurs between water oxygen and H<sub>11</sub>. Those linked to H<sub>15</sub> and H<sub>18</sub> have intermediate strength. The weakest between water hydrogen and O<sub>23</sub>. These four sites favour unstable bonds. They represent the degradation centres of α-D-glucose. This work analyzes potential complex between the monosaccharide and carbon dioxide.

**Citation:** Ablé Anoh Valentin, N'guessan Boka Robert and Bamba El-Hadji Sawaliho\*. Monosaccharide Degradation Analysis by Functional Density Theory at Level B3lyp/6-311 G (D, P).

Op Acc J Bio Sci & Res 6(2)-2020.

**DOI:** 10.46718/JBGSR.2020.06.000144

Table 4: AM1G- H<sub>2</sub>O Enthalpy Difference (Kcal mol<sup>-1</sup>) and its Variation in %.

ΔH (T)	ΔH (T1)	ΔH difference	ΔH Variation
-12,841	-12,841	0	0%
-9,981	-9,995	0.014	0%
-11,499	-11,501	0.002	0%
-7,307	-7.33	0.023	0%
Median		0.008	0%

Table 5: AM1G- H<sub>2</sub>O Free Enthalpy Difference (Kcal mol<sup>-1</sup>) and its Variation in %.

ΔG (T)	ΔG (T1)	ΔG difference	ΔG variation
-2,116	-2,553	0.437	21%
-1,217	-1,574	0.357	29%
-1,235	-1,653	0.418	34%
-1,497	-1,903	0.406	27%
Median		0.412	28%

### AM1G- CO<sub>2</sub> complex study

This section presents the geometric parameters of AM1G and [CO]<sub>2</sub>. To optimize them, the linearity angle α remains to 180°. β equals 120° with oxygen sp<sup>2</sup> hybridization. Calculations lead to the geometric parameters of the AM1G-CO<sub>2</sub>.

### Geometric Parameters

(Table 6) collects them. The distance d values range from 2.12 Å to 2.64 Å. They exceed that of the probe. They indicate no HB between the carbon dioxide's oxygen and AM1G's hydrogen. The direction and linearity angles support this finding. The temperature doesn't modify the geometric parameters of their possible complex.

Table 6: AM1G- CO<sub>2</sub> Geometric Parameters in kcal/mol.

Complex	T = 25 °C				T1 = 13 °C			
	d (Å)	α (°)	β (°)	θ (°)	d (Å)	α (°)	β (°)	θ (°)
AM1G (OH11)—CO <sub>2</sub>	2.12	166.90	131.45	177.45	2.12	166.87	131.46	177.46
AM1G (OH15)—CO <sub>2</sub>	2.21	147.01	122.72	178.21	2.21	147.00	122.71	178.21
AM1G (OH18)—CO <sub>2</sub>	2.64	100.26	94.43	177.25	2.64	100.26	94.43	177.25
AM1G (O23H)—CO <sub>2</sub>	2.81	139.28	69.49	177.45	2.81	139.28	69.49	177.45

### Energetic Parameters

Under these conditions, the geometric parameters prove that α-D glucose doesn't interact with carbon dioxide. The energy calculations allow testing this conjecture. (Table 7) resumes the values needed for this discussion.

Table 7: AM1G- CO<sub>2</sub> Energy Parameter in kcal/mol.

Complex	T= 25 °C				T1 =13 °C	
	Eélec	ΔEint	ΔH (T)	ΔG (T)	ΔH (T1)	ΔG (T1)
AM1G (OH <sub>11</sub> )—CO <sub>2</sub>	-549,727.082	-3,244	-4,544	3,843	-4,570	3,503
AM1G (OH <sub>15</sub> )—CO <sub>2</sub>	-549,725.364	-1,869	-2,911	4,640	-2,942	4,330
AM1G (OH <sub>18</sub> )—CO <sub>2</sub>	-549,725.808	-1,901	-3,461	3,724	-3,495	3,431
AM1G (O <sub>23</sub> H)—CO <sub>2</sub>	-549,727.082	-3,244	-4,544	3,847	-4,571	3,505

AM1G- CO<sub>2</sub> interaction energies vary between -1,869 and -3,244 kcal/mol. They're greater than those of the AM1G-OH<sub>2</sub> presented in (Table 3); the reaction between carbon dioxide and AM1G remains much lower. Enthalpy values ΔH suggest that that of AM1G- CO<sub>2</sub> be less exothermic. As shown in the (Table 8), on average, they decrease from 25 °C to 13 °C by 0.03 Kcal mol<sup>-1</sup>.

This difference is equivalent to 1% of the variation between the ambient and storage banana's temperatures. This magnitude remains negative; the complexation reaction stays exothermic in both situations. On average, free enthalpies decrease from 25 °C to 13 °C by 0.33 Kcal mol<sup>-1</sup> as presented in (Table 9). This difference is equivalent

Table 8: AM1G- CO<sub>2</sub> Enthalpy Difference (Kcal mol<sup>-1</sup>) and its Variation in %.

ΔH (T)	ΔH (T1)	ΔH différence	ΔH variation
-4,544	-4.57	0.026	1%
-2,911	-2,942	0.031	1%
-3,461	-3,495	0.034	1%
-4,544	-4,571	0.027	1%
Median		0.029	1%

Table 9: AM1G-CO<sub>2</sub> Free Enthalpy Difference (Kcal mol<sup>-1</sup>) and its Variation in %.

ΔG (T)	ΔG (T1)	ΔG différence	ΔG Variation
3,843	3,503	0.34	-9%
4.64	4.33	0.31	-7%
3,724	3,431	0.293	-8%
3,847	3,505	0.342	-9%
Median		0.325	-8%

**Citation:** Ablé Anoh Valentin, N'guessan Boka Robert and Bamba El-Hadji Sawaliho\*. Monosaccharide Degradation Analysis by Functional Density Theory at Level B3lyp/6-311 G (D, P).

Op Acc J Bio Sci & Res 6(2)-2020.

DOI: 10.46718/JBGSR.2020.06.000144

to an 8% variation between the ambient temperature and that of the banana storage. This magnitude stays positive; the reaction remains exothermic in both situations. Positive free energies show that complexation isn't spontaneous. Those of the electronic energies confirm the non-existence of hydrogen bonding; carbon dioxide interacts with AM1G with difficulty. Previous work imputes to it the capacity to slow the rotting of bananas. In this case, this research plans to examine its action on AM1G- H2O.

### AM1G- H2O-CO2 Complex Study

AM1G- H2O- CO2 investigation consists of analyzing its geometric and energy parameters. This work retains AM1G-OH2 optimized the first data. The d1 hypothetical distance (H26-O CO2 [29]) equals 2 Å. The linearity and direction angles between carbon dioxide and water are respectively  $\alpha$  (O25-H26-O29) = 180 ° and  $\beta$  (H26-O29-C28) = 120°. (Table 10) presents AM1G-OH2-CO2 spatial sizes.

Table 10: AM1G-OH2-CO2 Geometric Parameters.

Complex	T=25°C			T1=13°C		
	d(Å)	$\alpha$ (°)	$\beta$ (°)	d(Å)	$\alpha$ (°)	$\beta$ (°)
AM1G (OH <sub>11</sub> )-OH <sub>2</sub>	1.86	161.68	93.95	<b>1.86</b>	161.68	93.95
AM1G (OH <sub>15</sub> )-OH <sub>2</sub>	1.94	146.48	126.38	<b>1.94</b>	146.48	126.38
AM1G- (OH <sub>11</sub> )-OH <sub>2</sub> -CO <sub>2</sub>	1.89	160.09	92.83	<b>1.89</b>	160.1	92.83
AM1G- (OH <sub>15</sub> )-OH <sub>2</sub> -CO <sub>2</sub>	1.97	145.11	129.02	<b>1.97</b>	145.12	129.16

### Geometric Parameters

Linearity and direction angles are almost maintained; HB aren't subject to destabilizing torsion. This leads to say that in the presence of carbon dioxide, water hardly interacts with  $\alpha$ -D glucose. CO2. It reinforces the strength of its link with AM1G. It helps to equilibrate this latter. However, it remains to its liking in H11. Only the complex with H\_11 and H\_15 show variations in geometric parameters at room and stockade temperatures. For these two entities. (Table 10) data indicates that this doesn't modify AM1G-OH2- CO2. These information suggests collecting energetic ones.

### Energy Parameters

(Table 11) presents AM1G-H2O- CO2 energetic data. Carbon dioxide increase AM1G- H2O-CO2 interaction energy compared to that of AM1G- H2O. These high values indicate that the AM1G- H2O-CO2 becomes less stable than AM1G- H2O. CO2 enhance this latter complex's rigidity; it maintains HB within AM1G- H2O. Moreover, the positive

Table 11: AM1G- H2O- CO2 Energetic Parameters in kcal/mol.

Complex	T = 25 °C					T1 = 13 °C	
	Eélec	$\Delta E_{int}$	$\Delta E_{gap}$	$\Delta H$ (T)	$\Delta G$ (T)	$\Delta H$ (T1)	$\Delta G$ (T1)
AM1G(OH <sub>11</sub> )-OH <sub>2</sub> -CO <sub>2</sub>	-597,712.824	-1,398	169,722	-5,253	1,433	-15,287	0.753
AM1G(OH <sub>15</sub> )-OH <sub>2</sub> -CO <sub>2</sub>	-597,710.956	-0.153	178,746	-3,333	3,047	-13,369	2,380
AM1G(OH <sub>18</sub> )-OH <sub>2</sub> -CO <sub>2</sub>	-597,712.536	-0.477	177,371	-4,777	2,798	-15,287	0.753
AM1G(O <sub>23</sub> H)-OH <sub>2</sub> -CO <sub>2</sub>	-597,708.509	-7,232	178,288	-1,226	5,948	-11,285	5,217

free enthalpy ( $\Delta G$ ) illustrates the unpredictability of AM1G-H2O-CO2 formation. Furthermore, the enthalpies drop by 10.16 Kcal mol<sup>-1</sup>. It declines by almost 383% as shown in (Table 12). It continues to be negative; the complexation stay exothermic. On average, the free enthalpies decrease from 25 °C to 13 °C by 1.03 Kcalmol<sup>-1</sup> (Table 13). This variation is equivalent to a slowdown. It dips by 39% between the ambient temperature and that of its storage. It remains positive.

Table 12: AM1G-OH2- CO2 Enthalpy (Kcal mol<sup>-1</sup>) Difference and its Variation in %.

$\Delta H$ (T)	$\Delta H$ (T1)	$\Delta H$ difference	$\Delta H$ Variation
-5,253	-15,287	10,034	-191%
-3,333	-13,369	10,036	-301%
-4,777	-15,287	10.51	-220%
-1,226	-11,285	10,059	-820%
Median		10.15975	-383%

Table 13: AM1G-OH2- CO2 Free Enthalpy Difference (Kcal mol<sup>-1</sup>) and its Variation in %.

$\Delta G$ (T)	$\Delta G$ 1	$\Delta G$ difference	$\Delta G$ variation
1,433	0.753	0.68	47%
3,047	2.38	0.667	22%
2,798	0.753	2,045	73%
5,948	5,217	0.731	12%
Median		1.03075	39%

The reaction isn't spontaneous in both these two conditions. It tends towards its spontaneity when temperature decrease. Its enthalpy obeys the same trend. It indicates that HB creation stays exothermic. This variable doesn't modify this reaction thermodynamic properties. It

can't justify AM1 degradation. This explanation leads to the conclusion of the article.

## Conclusion

This work aims to identify the chemical modalities underlying the degradation of polysaccharides. Initially, it determines the relevant configuration of D-glucose anomer. It establishes that its alpha form is more stable than that of beta. The first quoted becomes the structure of AM1G here.

Furthermore, an ESP map analysis reveals AM1G polymerization centres. It demonstrates that the oxygen bound to the carbon of the anomeric ranks 1 or 2 and or in position 6 constitute these sites. The research examines the role of carbon dioxide and water in this process. The latter reagent produces a strong HB primarily between the H<sub>11</sub> and its oxygen. It establishes them with H<sub>18</sub> and H<sub>15</sub> of intermediate strength. It also participates in another through its hydrogen and O<sub>23</sub>. These bonds remain unstable. However, they contribute to the degradation of starch polysaccharides. On the other hand, this work establishes that carbon dioxide doesn't interact with  $\alpha$ -D-glucose. But it consolidates HB within the AM1G-H<sub>2</sub>O; it conserves its deterioration. Research refutes two conjectures.

The first concerns the part of temperature. The hypothetical complex formation shows its weak influence on reaction between  $\alpha$ -D-glucose-water and dioxide carbon. The change from room temper to that of the plantain storage doesn't modify compounds studied geometric parameters. It transforms the enthalpy and free enthalpy values of the AM1G- H<sub>2</sub>O-CO<sub>2</sub>. However, it doesn't impact on the exothermic and non-spontaneous nature of the AM1G- H<sub>2</sub>O complexation by CO<sub>2</sub>. This research aims to identify the chemical modalities underlying the degradation of polysaccharides.

The work mentions the role of carbon dioxide and water in this process. The latter reactant produces a strong HB primarily between the H<sub>11</sub> in the building block and its oxygen. It establishes them with H<sub>18</sub> and H<sub>15</sub> of intermediate strength. It participates in another through its hydrogen and O<sub>23</sub>. These links remain unstable. However, they contribute to the degradation of starch polysaccharides. Moreover, research highlights the lack of a relationship between the latter reactant action and its quantity. But this work doesn't exhaust saccharide potential deterioration sources. Analysis temperature effects on water or dioxide complex could clarify its influence on theses process. More, this study uses one amylum subunit. The chain extension to

several glucose can help to elucidate the two reactant roles on polysaccharide destruction.

## References

1. Rosales F (1998) Importance de production locale des bananiers plantains en Amérique latine et dans le caraïbe. *Banana and food society, INIBAP 2001*: 265-284.
2. Yao AK, Koffi DM, Irié ZB, Niamké SL (2014) Effet de la substitution partielle de la farine de blé par la purée de banane plantain (Musa AAB) bien mûre sur la qualité des produits de pâtisserie. *Journal of Applied Science 82*: 7436-7448.
3. FIRCA (2010) Répertoire de technologies de conservation et de transformation de l'igname et de la banane plantain. Fonds Interprofessionnel pour la Recherche et le Conseil Agricole. Groupe le prestige, Cocody-Abidjan.
4. Kerbel EL, Kader AA (1988) Effects of elevated CO<sub>2</sub> concentrations on glycolysis in intact "Barlett" pear fruit. *Plant Physiol 86*: 1205-1209.
5. Happi E, Bernard W (2008) Changement texturaux et biochimiques des fruits du bananier au cours de la maturation. Leur influence sur la préservation de la qualité du fruit et la maîtrise de la maturation. *Biotechnol. Agron. Soc. Environ 12(1)*: 89-98.
6. Cao Y, Wang YC (2004) Study on sugar profile of rice during ageing by capillary electrophoresis with electrochemical detection. *Food Chemistry 86*: 131-136.
7. Pathindol J, Wang, YJ, Jane J (2005) Structure-Functionality Changes in Starch Following Rough Rice Storage. *Starch-Stärke 57*: 197-207.
8. Choehom R, Kesta S (2004) senescent spotting of banana peel is inhibited by 8 modified atmosphere packaging. *Postharvest Biol. Technol 31*: 167-175.
9. Trakulnaleumsai C, Kesta S (2006) Temperature effects on peel spotting in sucrier banana fruit. *Postharvest Biol. Technol 39*: 285-290.
10. Frisch GW, Schlegel GE, Robb JR, Scalmani V, Mennucci GA, et al. (2008) Gaussian 09, Revision A.02. *Coordination Chemistry Reviews 252(3)*: 395-415.
11. Hohenberg P, Kohn W (1964) Inhomogeneous electron gas. *Phys. Rev 136*: 864.
12. Evangelisti L, Feng G, Gou Q, Grabow JU, Caminati W (2014) Halogen Bond and Free Internal Rotation: The Microwave spectrum of CF<sub>3</sub>Cl-Dimethyl Ether. *J. Phys. Chem A 118(13)*: 579-582.
13. Ziao N, Le Questel JY, YN (2005) Caractérisation énergétique des sites de fixation de liaison hydrogène dans les aminonitriles par la méthode de la fonctionnelle de la densité. *J. Soc Ouest-Afr. Chim 20*: 101-118.
14. Desiraju GR (2011) Reflections on the Hydrogen Bond in Crystal Engineering. *Crystal Growth & Design 11(4)*: 896-898.
15. Ziao N, Craton J, Laurence C, Le Questel JY (2001) Amino and cyano N atoms in competitive situations : which is the best hydrogen-bond acceptor? *Acta Crystallogr., Sect. B : Struct. Sci, B 57*: 850-858.
16. Reed AE, Weinstock RB, Winhold F (1985) Natural population analysis. *The Journal of Chemical Physics 83(12)*: 735-782.

**Citation:** Ablé Anoh Valentin, N'guessan Boka Robert and Bamba El-Hadji Sawaliho\*. Monosaccharide Degradation Analysis by Functional Density Theory at Level B3lyp/6-311 G (D, P).

*Op Acc J Bio Sci & Res 6(2)*-2020.

**DOI:** 10.46718/JBGSR.2020.06.000144



- 
17. Kadjo KF, Koné GRM, Sopi AT, Ziao N (2017) Oniom method characterisation of hydrogen bonding sites of mycolactone A/B, a Burli Ulcer Toxin. Computational Chemistry 5: 103-112.
  18. Vidal J (1997) Thermodynamique : application au génie chimique et à l'industrie pétrolière. . Editions TECHNIP.
  19. Alberty RA (2001) Use of Legendre transforms in chemical thermodynamics (IUPAC Technical Report). Pure and Applied Chemistry 73(8): 1349-1380.
  20. Momany FA, Appell M, Strati G (2004) B3LYP/6311++G\*\* study of monohydrates of a- and b-Dglucopyranose: hydrogen bonding, stress energies, and effect of hydration on internal coordinates. Carbohydrate Research 339: 553-567.

\*Corresponding author: Bamba El-Hadji Sawaliho, Email: bamba\_el\_hadji@yahoo.fr

Next Submission with BGSR follows:

- Rapid Peer Review
- Reprints for Original Copy
- E-Prints Availability
- Below URL for auxiliary Submission Link: <https://biogenericpublishers.com/submit-manuscript/>